

## Electronic Supplementary Information

### **Catalytic activity atlas of ternary Co-Fe-V metal oxides for oxygen evolution reaction**

Junsheng Chen<sup>a</sup>, Hao Li<sup>b</sup>, Zengxia Pei<sup>a</sup>, Qianwei Huang<sup>c</sup>, Ziwen Yuan<sup>a</sup>, Chaojun Wang<sup>a</sup>, Xiaozhou Liao<sup>c</sup>, Graeme Henkelman<sup>b</sup>, Yuan Chen<sup>a,\*</sup> and Li Wei<sup>a,\*</sup>

<sup>a</sup> School of Chemical and Biomolecular Engineering, The University of Sydney, Sydney, New South Wales, 2006, Australia

<sup>b</sup> Department of Chemistry and the Oden Institute for Computational and Engineering Sciences, The University of Texas at Austin, 105 E. 24th Street, Stop A5300, Austin, Texas, United States, 78712

<sup>c</sup> School of Aerospace, Mechanical and Mechatronic Engineering, The University of Sydney, Sydney, New South Wales, 2006, Australia

Authors emails: [yuan.chen@sydney.edu.au](mailto:yuan.chen@sydney.edu.au) (Y. C.) and [l.wei@sydney.edu.au](mailto:l.wei@sydney.edu.au) (L.W)

**Table S1.** Amount of Co, Fe and V precursor used for synthesising different CoFeV PBA precursors.

Sample No.	Designed composition			Precursor volume, mL					
	Co	Fe	V	CoCl <sub>2</sub> (50 mM)	FeCl <sub>2</sub> (50 mM)	VOSO <sub>4</sub> (50 mM)	H <sub>2</sub> O	K <sub>3</sub> [Fe(CN) <sub>6</sub> ] (20 mM)	K <sub>3</sub> [Co(CN) <sub>6</sub> ] (20 mM)
1	2	6	2	10	10	10	20	50	0
2	1	6	3	5	10	15	20	50	0
3	3.33	5	1.67	16.65	5	8.35	20	50	0
4	1.67	5	3.33	8.35	5	16.65	20	50	0
5	1	5	4	5	5	20	20	50	0
6	4.5	4	1.5	22.5	0	7.5	20	50	0
7	4	4	2	20	0	10	20	50	0
8	3	4	3	15	0	15	20	50	0
9	2	4	4	10	0	20	20	50	0
10	1.5	4	4.5	7.5	0	22.5	20	50	0
11	1	4	5	5	0	25	20	50	0
12	5	3	2	20	0	10	20	37.5	12.5
13	4.67	3	2.33	18.35	0	11.65	20	37.5	12.5
14	3.5	3	3.5	12.5	0	17.5	20	37.5	12.5
15	6	2	2	10	10	10	20	0	50
16	5.33	2	2.67	16.65	0	13.35	20	25	25
17	2.67	2	5.33	3.35	0	26.65	20	25	25
18	0	10	0	0	30	0	20	50	0
19	0	8	2	0	20	10	20	50	0
20	0	7	3	0	15	15	20	50	0
21	0	5	5	0	5	25	20	50	0
22	0	4	6	0	0	30	20	50	0
23	2	8	0	10	20	0	20	50	0
24	4	6	0	0	30	0	20	0	50
25	6	4	0	30	0	0	20	50	0
26	8	2	0	30	0	0	20	25	25
27	10	0	0	30	0	0	20	0	50
28	8	0	2	20	0	10	20	0	50
29	5	0	5	5	0	25	20	0	50
30	4	0	6	0	0	30	20	0	50

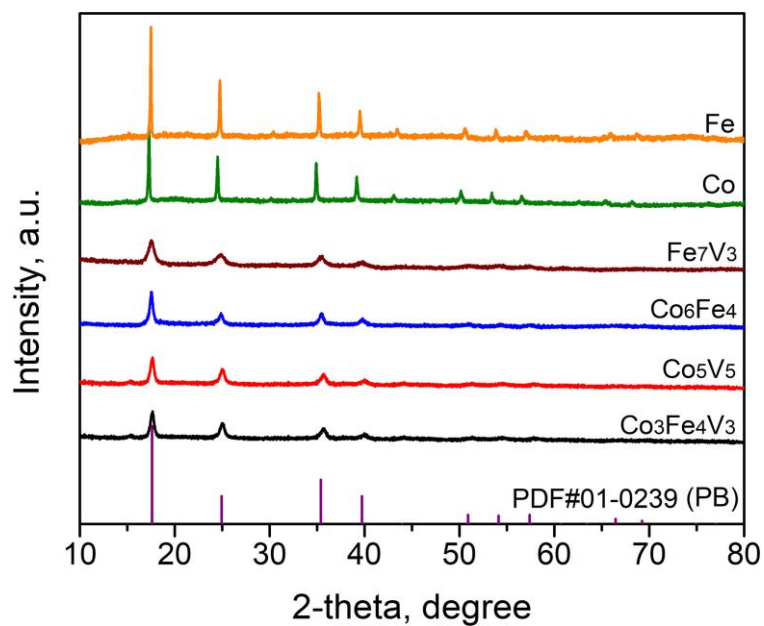


**Fig. S1** XRD patterns of different PBA nanoparticles synthesized in this study.

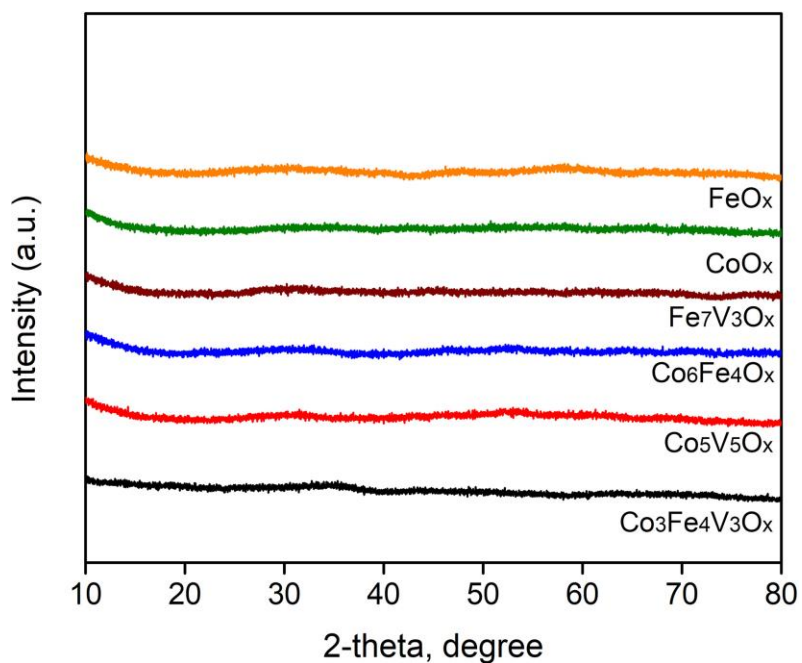


**Fig. S2** XRD patterns of metal oxides synthesized in this study.

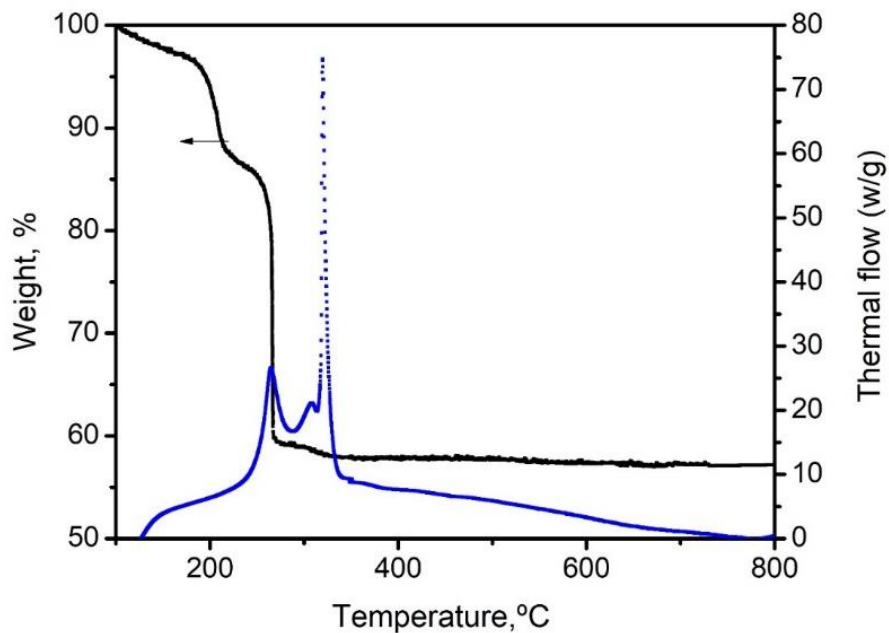


**Fig. S3** TGA and thermal flow profile of  $\text{Co}_3\text{Fe}_4\text{V}_3$  PBA nanoparticles.

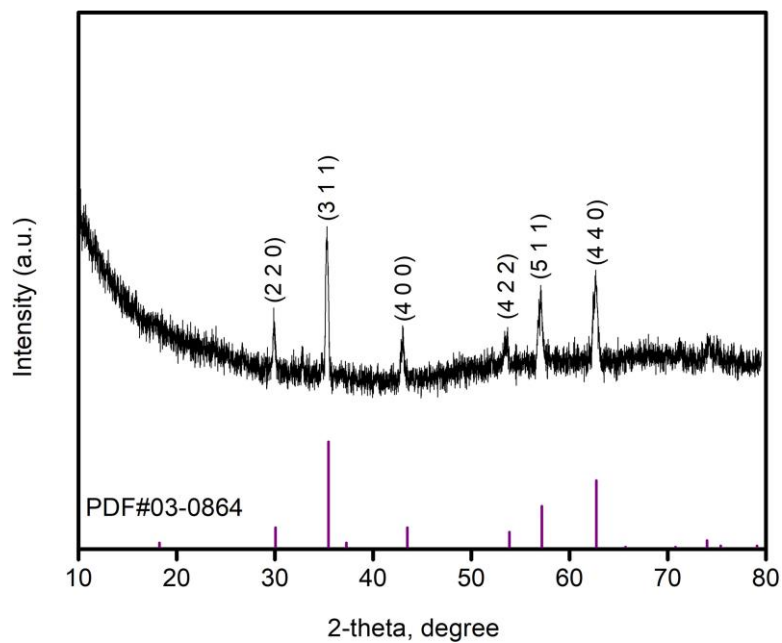


**Fig. S4** XRD patterns of  $\text{Co}_3\text{Fe}_4\text{V}_3\text{O}_x$  nanoparticles obtained after thermally decomposing PBA nanoparticles in the air at 350 °C. Standard lines of a spinel  $\text{CoFe}_2\text{O}_4$  (PDF#03-0864) is displayed for comparison.

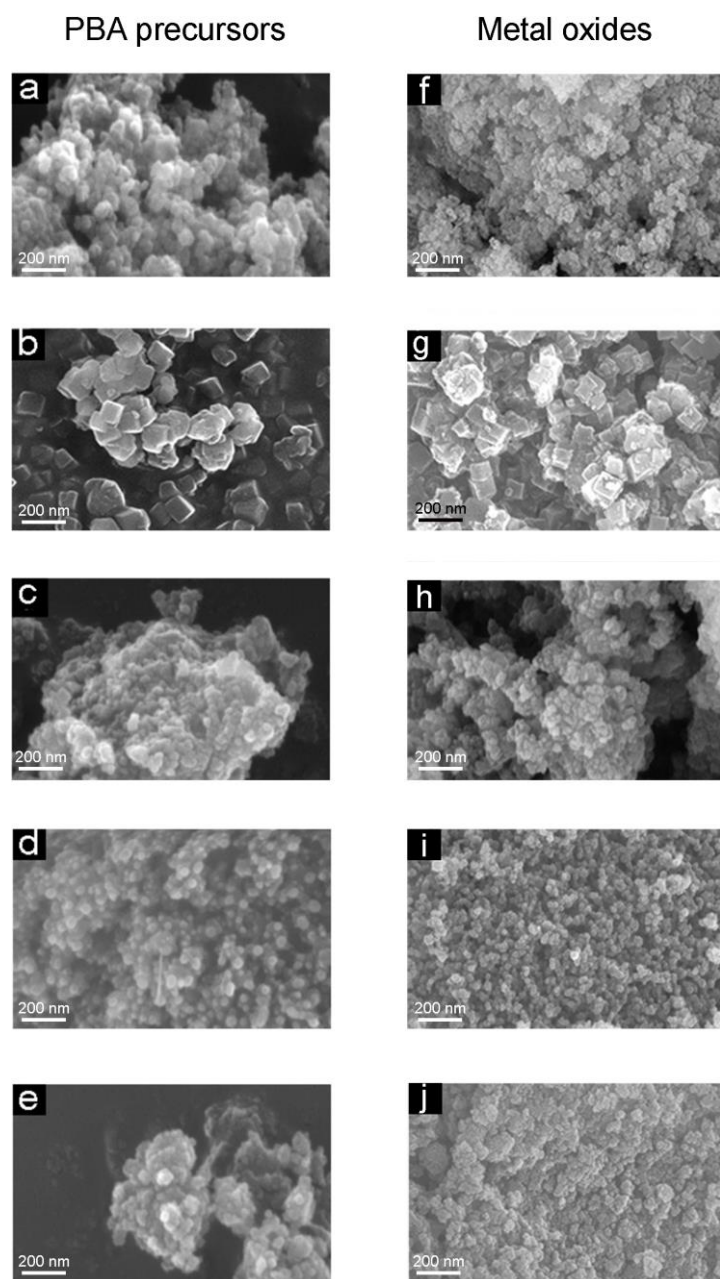


**Fig. S5** SEM images of various PBA nanoparticles and their corresponding metal oxide nanoparticles. (a) and (f)  $\text{Co}_6\text{V}_4$ , (b) and (g)  $\text{Co}$ , (c) and (h)  $\text{Fe}_7\text{V}_3$ , (d) and (i)  $\text{Co}_6\text{Fe}_4$ , (e) and (j)  $\text{Fe}$ .

**Table S2.** Particle size of various PBA precursors and their derived metal oxide particles determined by SEM

	Diameter of PBA precursor, nm	Diameter of metal oxide, nm
$\text{Co}_3\text{Fe}_4\text{V}_3$	$53.91 \pm 4.35$	$49.57 \pm 7.26$
$\text{Co}_6\text{V}_4$	$65.78 \pm 5.43$	$60.05 \pm 9.19$
$\text{Co}$	$96.53 \pm 10.93$	$87.20 \pm 7.92$
$\text{Fe}_7\text{V}_3$	$69.38 \pm 6.92$	$53.20 \pm 6.09$
$\text{Co}_6\text{Fe}_4$	$51.50 \pm 4.87$	$49.43 \pm 5.40$
$\text{Fe}$	$62.16 \pm 9.47$	$60.38 \pm 6.48$

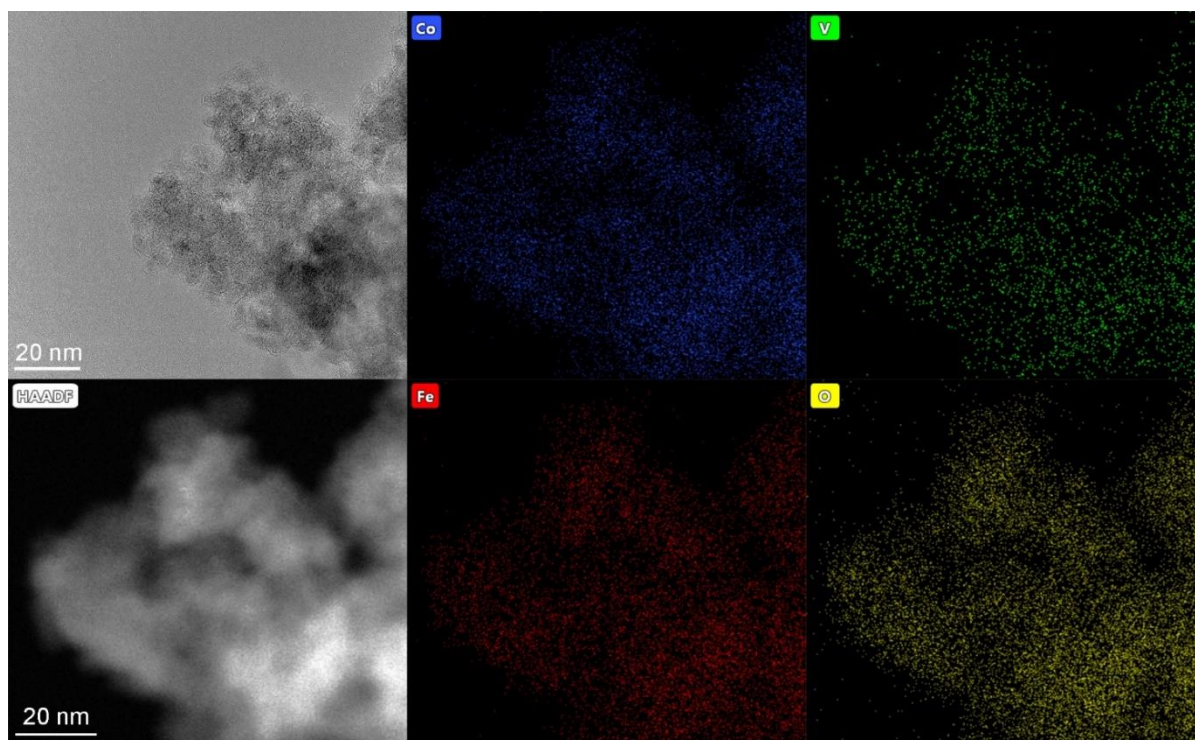


**Fig. S6** TEM and HAADF-STEM EDX elemental mappings of  $\text{Co}_3\text{Fe}_4\text{V}_3$  PBA nanoparticles.

**Table S3.** Elemental compositions (in molar ratio) of Co-Fe-V metal oxides determined by different methods.

	Designed			EDX			ICP-AES			XPS		
	Co	Fe	V	Co	Fe	V	Co	Fe	V	Co	Fe	V
$\text{Co}_3\text{Fe}_4\text{V}_3\text{O}_x$	3	4	3	2.90	3.99	3.11	2.97	4.09	3.04	2.85	3.96	3.19
$\text{Co}_5\text{V}_5\text{O}_x$	5	0	5	5.03	0.00	4.97	5.11	0.00	4.89	5.16	0.00	4.84
$\text{Co}_6\text{Fe}_4\text{O}_x$	6	4	0	5.93	4.07	0.00	5.88	4.12	0.00	6.06	3.95	0.00
$\text{Fe}_7\text{V}_3\text{O}_x$	0	7	3	0.00	2.89	7.11	0.00	7.07	2.93	0.00	6.95	3.05

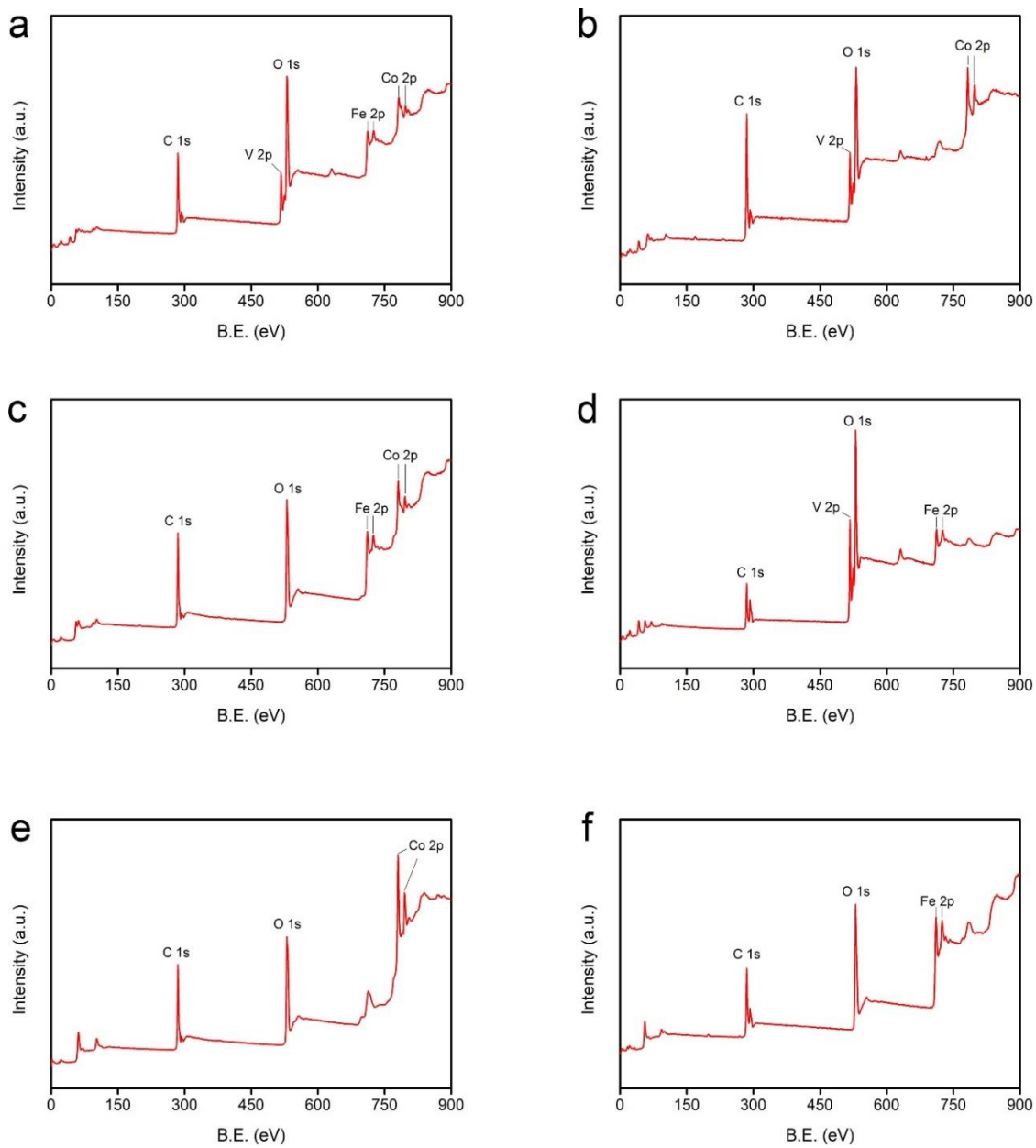


**Fig. S7** XPS survey spectra of (a)  $\text{Co}_3\text{Fe}_4\text{V}_3\text{O}_x$ , (b)  $\text{Co}_5\text{V}_5\text{O}_x$ , (c)  $\text{Co}_6\text{Fe}_4\text{O}_x$ , (d)  $\text{Fe}_7\text{V}_3\text{O}_x$ , (e)  $\text{CoO}_x$ , and (f)  $\text{FeO}_x$  samples.

**Table S4.** OER performance of Co-Fe-V metal oxide samples tested in this study.

Sample No.	Designed composition (molar ratio)			Experimental composition (molar ratio) <sup>a</sup>				$\eta_{10}$ , mV	Tafel slope, mV dec <sup>-1</sup>
	Co	Fe	V	Co	Fe	V	O <sup>b</sup>		
1	2	6	2	1.94	5.95	2.11	14.71	396	70
2	1	6	3	0.94	6.08	2.98	14.91	419	80
3	3.33	5	1.67	3.09	4.97	1.94	14.23	335	68
4	1.67	5	3.33	1.50	4.97	3.53	15.01	398	67
5	1	5	4	0.94	5.04	4.02	15.13	412	67
6	4.5	4	1.5	4.57	4.08	1.36	13.78	334	74
7	4	4	2	3.78	3.96	2.26	13.60	343	60
8	3	4	3	2.85	3.96	3.19	14.43	249	41
9	2	4	4	1.87	4.07	4.06	15.38	279	63
10	1.5	4	4.5	1.60	4.11	4.29	16.01	292	66
11	1	4	5	0.90	3.95	5.15	16.56	385	74
12	5	3	2	4.89	3.03	2.09	14.13	345	55
13	4.67	3	2.33	4.54	3.07	2.39	13.79	296	47
14	3.5	3	3.5	3.22	2.95	3.82	14.73	287	51
15	6	2	2	5.90	1.93	2.17	14.31	342	62
16	5.33	2	2.67	5.46	1.96	2.58	14.92	313	59
17	2.67	2	5.33	2.82	1.86	5.32	16.31	335	72
18	0	10	0	0.00	10	0.00	14.59	656	153
19	0	8	2	0.00	8.15	1.85	14.74	567	112
20	0	7	3	0.00	6.95	3.05	14.58	519	78
21	0	5	5	0.00	5.10	4.90	16.16	531	87
22	0	4	6	0.00	4.11	5.89	15.99	589	105
23	2	8	0	2.06	7.94	0.00	15.19	458	97
24	4	6	0	4.09	5.91	0.00	14.69	412	71
25	6	4	0	6.06	3.95	0.00	15.13	345	63
26	8	2	0	8.11	1.89	0.00	14.25	372	70
27	10	0	0	10	0.00	0.00	14.59	386	77
28	8	0	2	7.83	0.00	2.17	15.41	369	65
29	5	0	5	5.16	0.00	4.84	15.23	319	56
30	4	0	6	3.87	0.00	6.13	15.85	359	78

a. Determined by ICP-AES measurements.

b. Determined from XPS survey scan. This value is also the x value in different Co<sub>a</sub>Fe<sub>b</sub>V<sub>c</sub>O<sub>x</sub> samples.

**Table S5.** Performance comparison of recently reported OER electrocatalysts based on Co, Fe and V oxides.

Sample	Substrate	Electrolyte	$\eta_{10}$ , mV	Tafel slope, mV dec <sup>-1</sup>	Ref.
Co <sub>3</sub> Fe <sub>4</sub> V <sub>3</sub> O <sub>x</sub>	GCE	1 M KOH	249	41	This work
CoV <sub>1.5</sub> Fe <sub>0.5</sub> O <sub>4</sub>	GCE	1 M KOH	300	38	<i>ACS Catal.</i> , <b>2018</b> , 8, 1259
V-Co-Fe-343(souce)	GCE	1 M KOH	307	36	<i>J. Mater. Chem. A</i> , <b>2015</b> , 3, 17763
$\alpha$ -CoVO <sub>x</sub>	GCE	1M KOH	347	51	<i>ACS Catal.</i> , <b>2018</b> , 8, 644
CoO <sub>x</sub> + Fe <sup>3+</sup>	GCE	1M KOH	309	27.6	<i>ACS Catal.</i> , <b>2017</b> , 8, 807
Fe <sub>0.5</sub> V <sub>0.5</sub> OOH	GCE	1M KOH	390	36.7	<i>Angew. Chem. Int. Ed.</i> , <b>2017</b> , 56, 3289
VOOH-3Fe	GCE	1M KOH	195	55	<i>Small</i> , <b>2019</b> , 15, 1904688
Co <sub>3</sub> O <sub>4</sub> /Co-Fe Oxide	GCE	1M KOH	297	61	<i>Adv. Mater.</i> <b>2018</b> , 30, 1801211
$\alpha$ -Co <sub>4</sub> Fe(OH) <sub>x</sub>	GCE	1M KOH	295	52	<i>J. Mater. Chem. A</i> , <b>2017</b> , 5, 1078
Co/Fe 15	GCE	0.1M KOH	390	61	<i>J. Mater. Chem. A</i> , <b>2017</b> , 5, 6849
CoFe35 LDH	GCE	0.1M KOH	350	49	<i>ChemSusChem</i> , <b>2017</b> , 10, 156
Fe1Co1-ONS	GCE	1M KOH	308	36.8	<i>Adv. Mater.</i> , <b>2017</b> , 29, 1606793
CoFe2O4	GCE	1M KOH	266	53	<i>Appl. Catal. B</i> , <b>2019</b> , 245, 1
WCoFex-CNF	Ni Foam	1M KOH	254	44.8	<i>Small</i> , <b>2019</b> , 15, 1901940
CoFe-H	Graphite	1M KOH	280	28	<i>Adv. Funct. Mater.</i> , <b>2017</b> , 27, 1603904
Co-Fe	Carbon paper	1M KOH	330	37	<i>Electrochimi Acta</i> , <b>2018</b> , 260, 872
CoFe	Carbon paper	1M KOH	283	51	<i>Nano Energy</i> , <b>2017</b> , 53, 576
CoFeV LDH/NF	Ni Foam	1 M KOH	242	57	<i>ACS Sustain. Chem. Eng.</i> , <b>2019</b> , 7 16828
Co <sub>0.8</sub> V <sub>0.2</sub> OOH	Ni foam	1M KOH	190	39.6	<i>J. Mater. Chem. A</i> , <b>2019</b> , 7 21911
CoV-UAH	Au foam	1M KOH	215	-	<i>Energy Environ. Sci.</i> , <b>2018</b> , 11 1736
Fe-Co <sub>3</sub> O <sub>4</sub> H-NSs/NF	Ni foam	1M KOH	204	38	<i>Nano Energy</i> , <b>2018</b> , 54, 238
CoFe/NF	Ni foam	1M KOH	220	40	<i>Small</i> , <b>2018</b> , 14, 1702568
FCCH/NF	Ni foam	1M KOH	228		<i>Adv. Energy Mater.</i> <b>2018</b> , 8, 1800175
CoFe PBA-2h	Ni foam	1M KOH	274	53	<i>Adv. Energy Mater.</i> <b>2018</b> , 8, 1800085

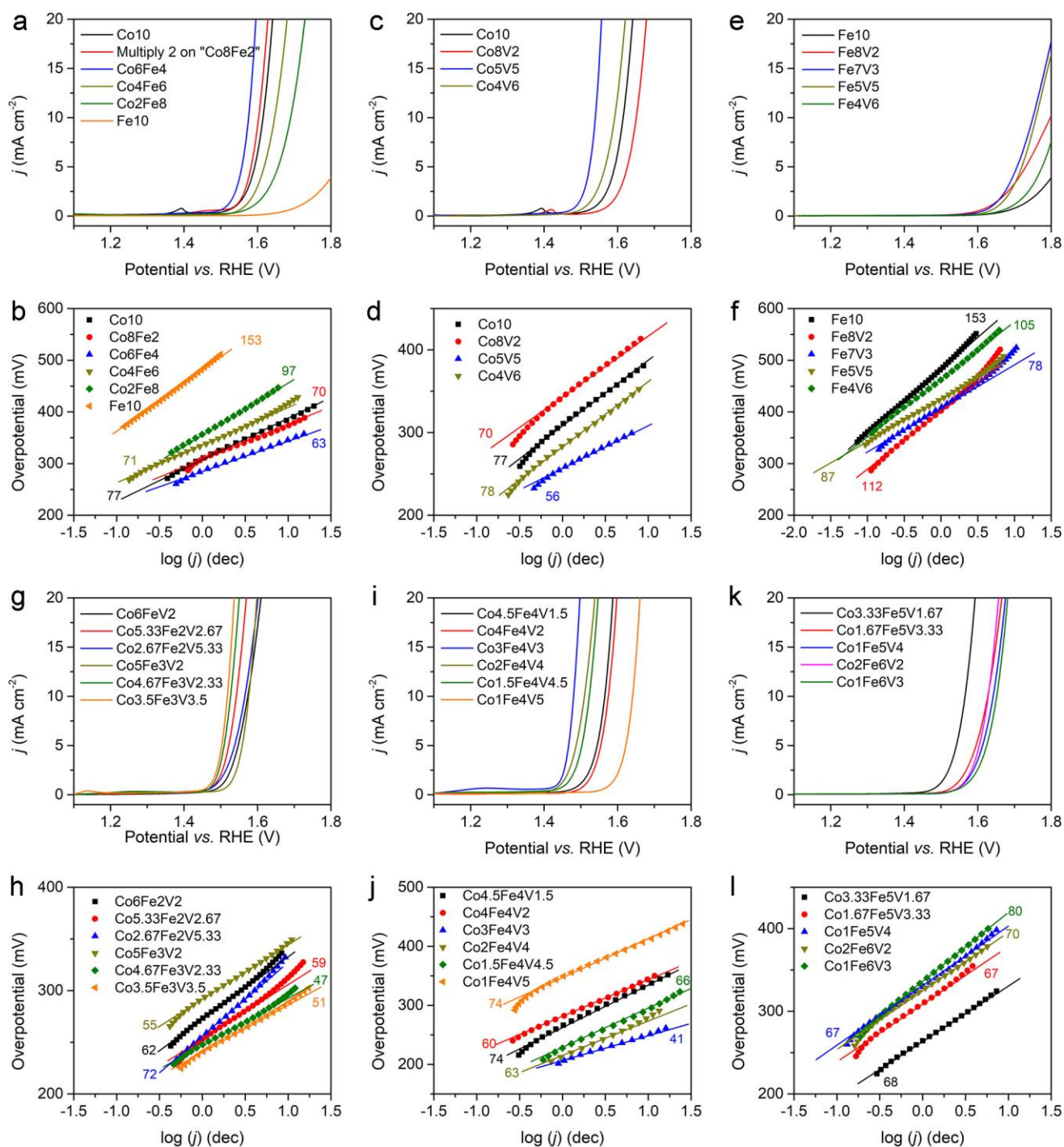


**Fig. S8** OER LSV and Tafel plots of tested  $\text{Co}_a\text{Fe}_b\text{V}_c\text{O}_x$  samples. (a) & (b) Co-Fe samples; (c) & (d) Co-V samples; (e) & (f) Fe-V samples; (g) & (h)  $\text{Co}_a\text{Fe}_2\text{V}_c\text{O}_x$  and  $\text{Co}_a\text{Fe}_3\text{V}_c\text{O}_x$  samples; (i) & (j)  $\text{Co}_a\text{Fe}_4\text{V}_c\text{O}_x$  samples (k) & (l)  $\text{Co}_a\text{Fe}_5\text{V}_c\text{O}_x$  and  $\text{Co}_a\text{Fe}_6\text{V}_c\text{O}_x$  samples.

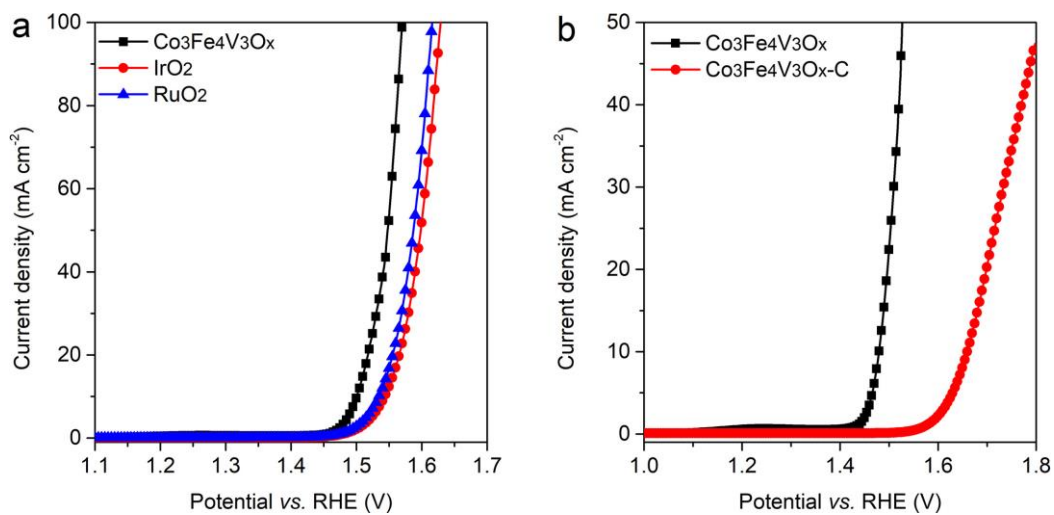


**Fig. S9** LSV curves of Co<sub>3</sub>Fe<sub>4</sub>V<sub>3</sub>O<sub>x</sub> in comparison to (a) IrO<sub>2</sub> and RuO<sub>2</sub> benchmarks and (b) phase-segregated Co<sub>3</sub>Fe<sub>4</sub>V<sub>3</sub>O<sub>x</sub>-C sample.

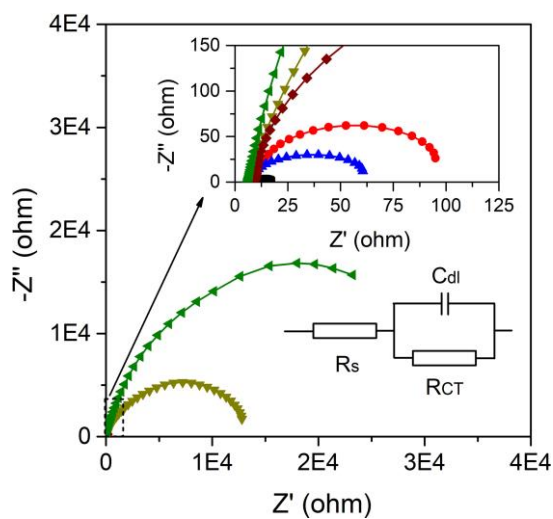


**Fig. S10** Full ESI Nyquist plots of different samples and the equivalent circuit.

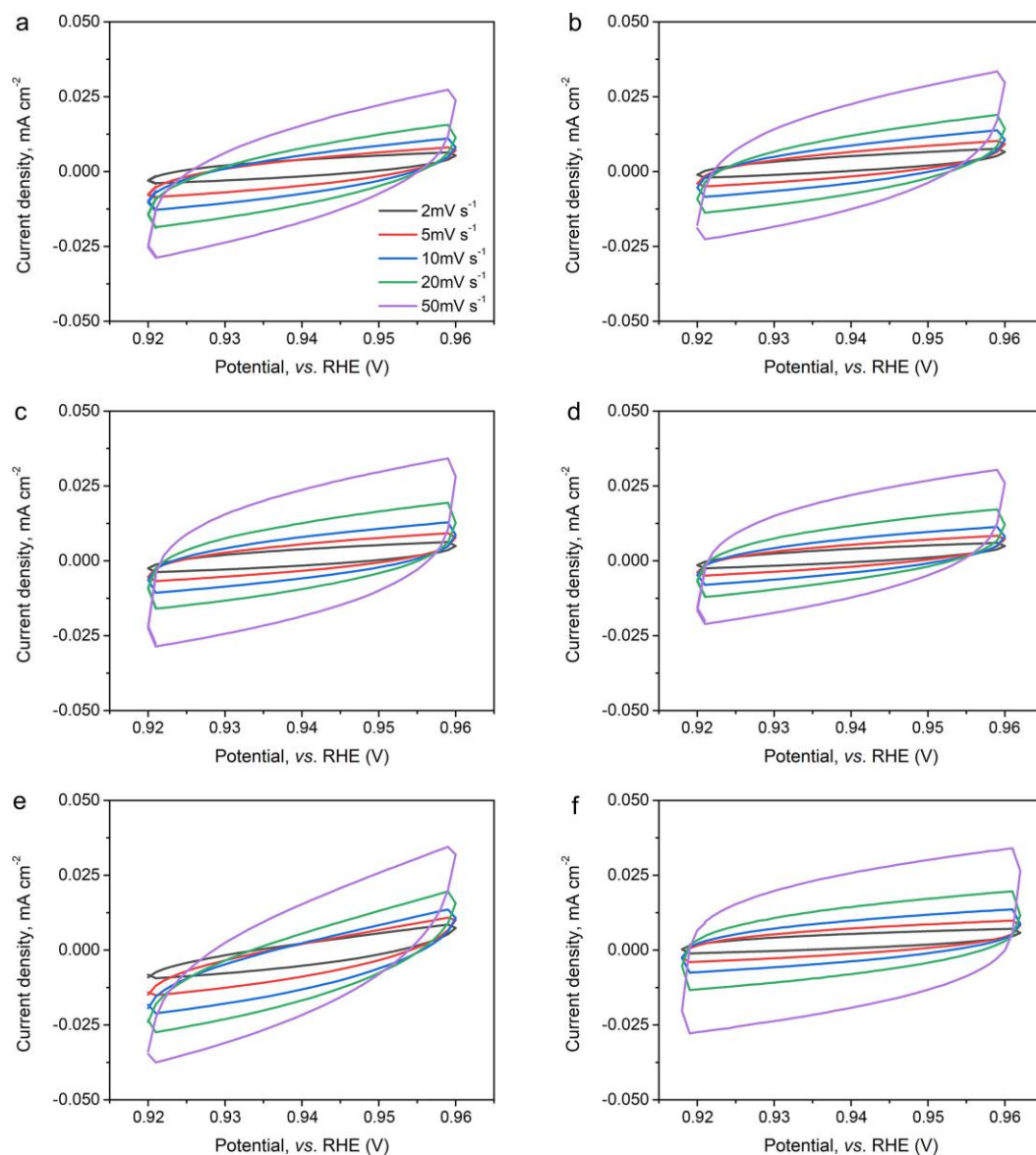


**Fig. S11** CV curves of (a)  $\text{Co}_3\text{Fe}_4\text{V}_3\text{O}_x$ , (b)  $\text{Co}_5\text{V}_5\text{O}_x$ , (c)  $\text{Co}_4\text{Fe}_6\text{O}_x$ , (d)  $\text{Fe}_7\text{V}_3\text{O}_x$ , (e)  $\text{CoO}_x$ , and (f)  $\text{FeO}_x$  samples collected at different scan rates.

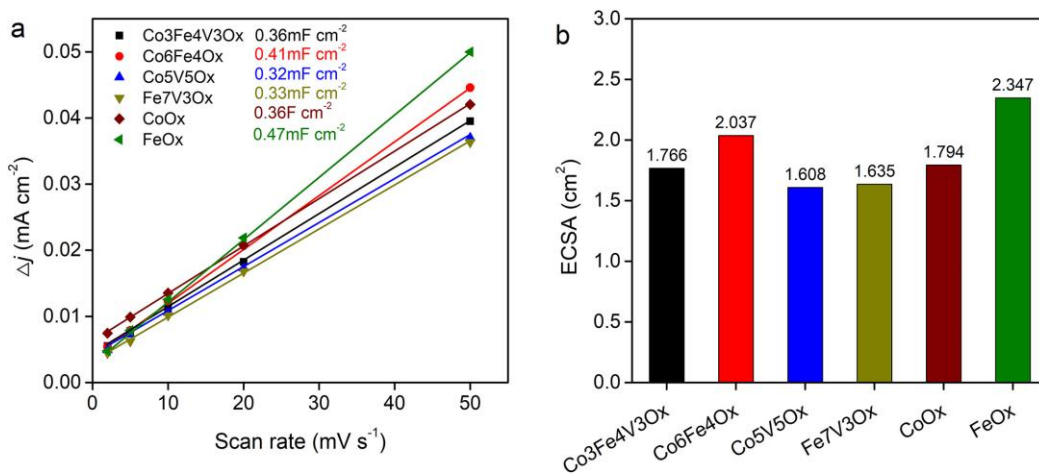


**Fig. S12** (a)  $\Delta j$  (0.94 V vs. RHE) plotted against scan rate and the calculated  $C_{dl}$  and (b) calculated ECSA of different Co-Fe-V metal oxide samples.

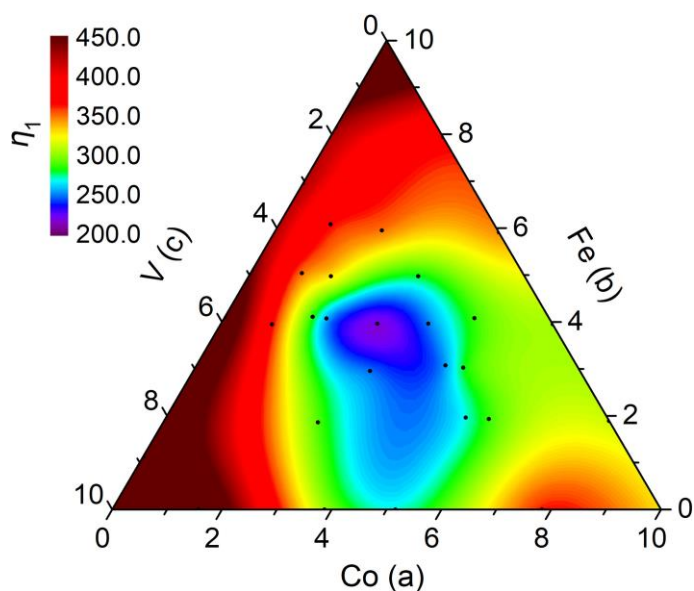


**Fig. S13** OER performance atlas of ternary  $Co_aFe_bV_cO_x$  based on the overpotential required to reach a  $j_{ECSA}$  of 1 mA cm<sup>-2</sup>. Sample compositions were determined by ICP-AES and marked by black dots.

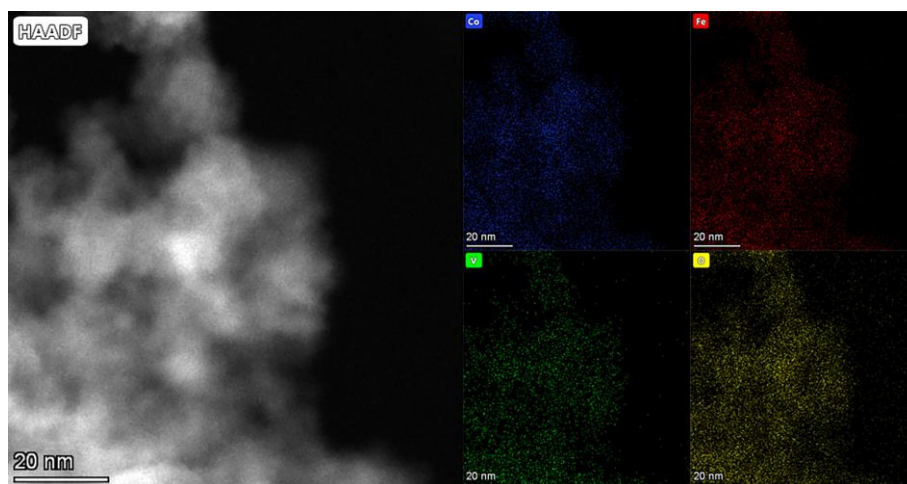


**Fig. S14** A TEM image of  $\text{Co}_3\text{Fe}_4\text{V}_3\text{O}_x$  after the 72-hour OER stability test (left) and the corresponding EDX elemental mappings of Co, Fe, V, and O (right).

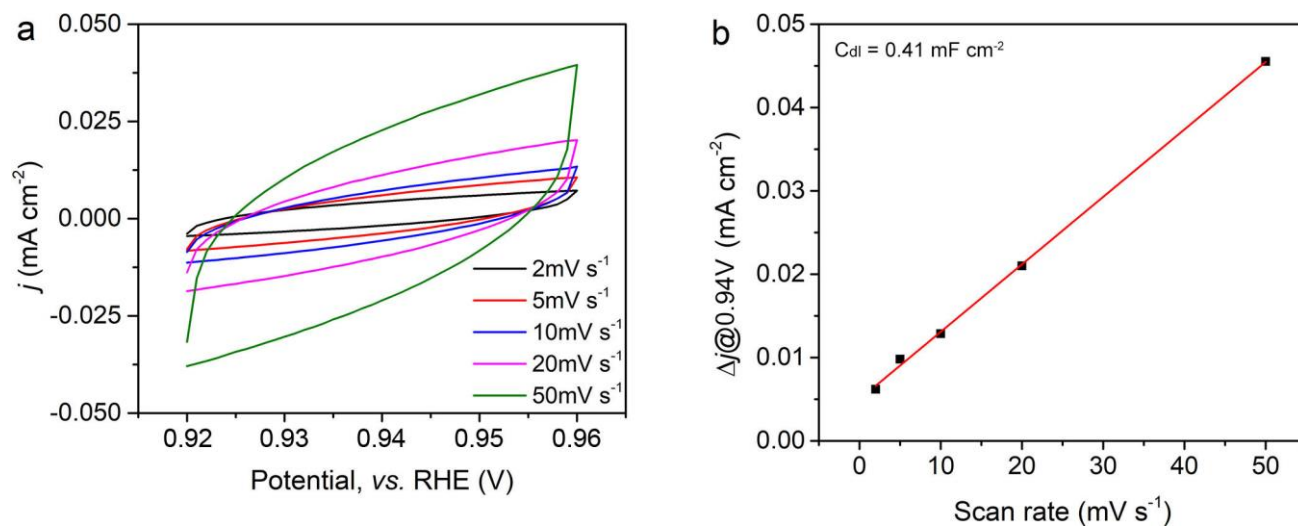


**Fig. S15** (a) CV curves obtained at different scan rates and (b)  $\Delta j@0.94\text{V}$  plotted against scan rates of the  $\text{Co}_3\text{Fe}_4\text{V}_3\text{O}_x$  after the OER stability test.

**Table S6.** Theoretical and experimental onset potential of different samples.

Catalyst	Onset overpotential (V)	
	Theoretical values	Experimental values ( $\eta_{\text{ECSA-0.25}}$ )
Co-CoFeV (near Fe)	0.63	0.19
Co-CoFeV (near V)	1.12	
Co-CoV	0.77	0.28
Co-CoFe	0.87	0.29
Co	0.94	0.35

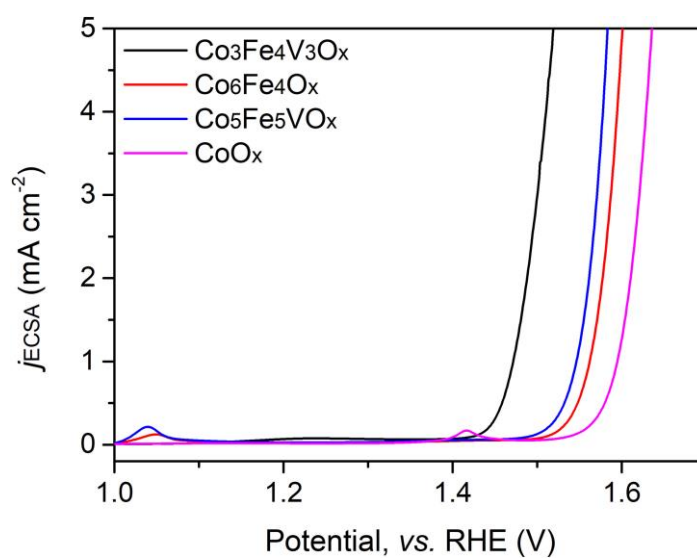


**Fig. S16** ECSA normalized LSV curves of different samples.

**Table S7.** Metal valence contents (at%) in different  $\text{Co}_a\text{Fe}_b\text{V}_c\text{O}_x$  determined from their high-resolution XPS spectra.

	<b>Co<sup>2+</sup></b>	<b>Co<sup>3+</sup></b>		<b>Fe<sup>2+</sup></b>	<b>Fe<sup>3+</sup></b>		<b>V<sup>3+</sup></b>	<b>V<sup>4+</sup></b>	<b>V<sup>5+</sup></b>	
Position, eV	781.9	779.9		710.2	711.2		515.6	516.7	517.8	
<b>Catalyst</b>	<b>Co<sup>2+</sup></b>	<b>Co<sup>3+</sup></b>	<b>Co average valence</b>	<b>Fe<sup>2+</sup></b>	<b>Fe<sup>3+</sup></b>	<b>Fe average valence</b>	<b>V<sup>3+</sup></b>	<b>V<sup>4+</sup></b>	<b>V<sup>5+</sup></b>	<b>V average valence</b>
<b>Co<sub>3</sub>Fe<sub>4</sub>V<sub>3</sub>O<sub>x</sub></b>	<b>73.9</b>	<b>26.1</b>	<b>2.261</b>	<b>18.7</b>	<b>81.3</b>	<b>2.813</b>	<b>13.2</b>	<b>62.3</b>	<b>24.5</b>	<b>4.114</b>
Co <sub>5</sub> Fe <sub>4</sub> V <sub>1</sub> O <sub>x</sub>	47.6	52.4	2.524	22.0	78.0	2.780	4.7	73.2	22.1	4.174
Co <sub>1</sub> Fe <sub>4</sub> V <sub>5</sub> O <sub>x</sub>	77.7	22.3	2.223	14.1	85.9	2.859	10.4	84.7	5.0	3.946
Co <sub>6</sub> Fe <sub>4</sub> O <sub>x</sub>	48.6	51.4	2.514	24.2	75.8	2.758	-	-	-	-
Co <sub>5</sub> V <sub>5</sub> O <sub>x</sub>	89.6	10.4	2.104	-	-	-	4.1	69.4	26.5	4.224
Fe <sub>7</sub> V <sub>3</sub> O <sub>x</sub>	-	-	-	3.4	96.6	2.966	15.4	76.5	8.0	3.926
CoO <sub>x</sub>	41.3	58.7	2.587	-	-	-	-	-	-	-
FeO <sub>x</sub>	-	-	-	25.8	74.2	2.742	-	-	-	-

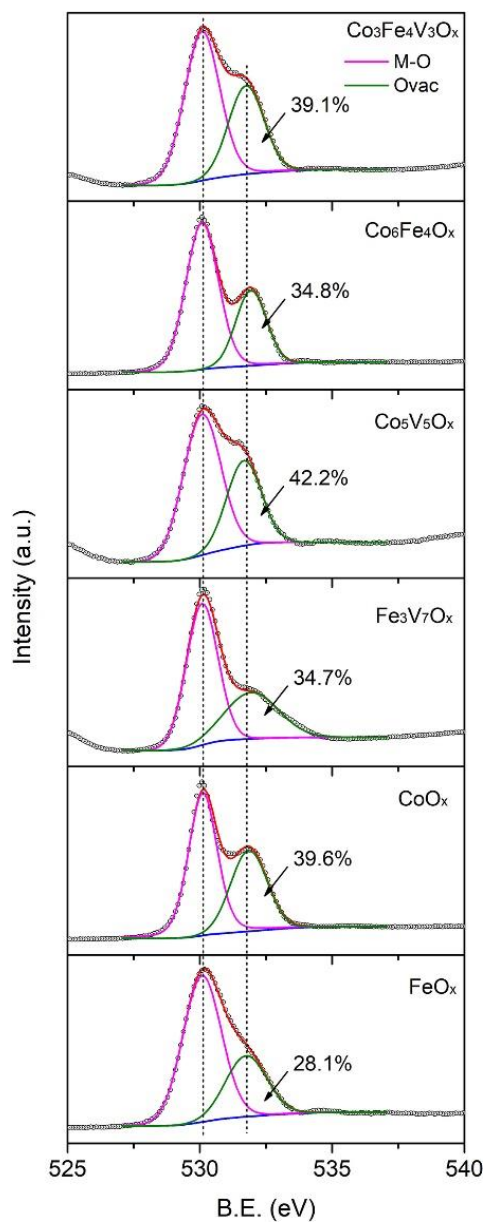


**Fig. S17** O1s XPS spectra of different samples.

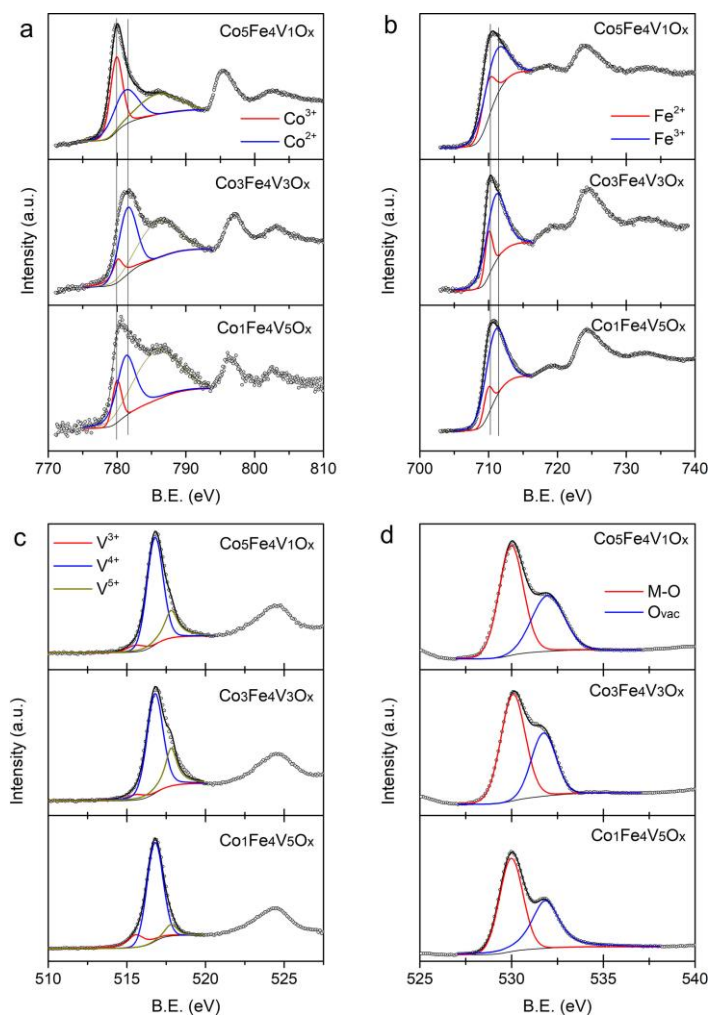


**Fig. S18** XPS spectra of (a) Co, (b) Fe, (c) V and (d) O in  $\text{Co}_1\text{Fe}_4\text{V}_5\text{O}_x$  (top panels) and  $\text{Co}_5\text{Fe}_4\text{V}_1\text{O}_x$  (bottom panels) samples.

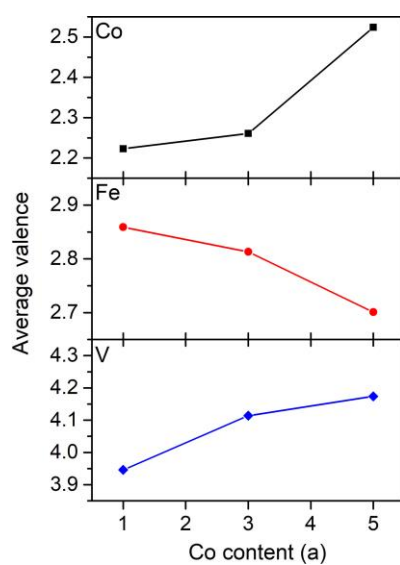


**Fig. S19** The relationship between average valence states of different metals and the abundance of Co in various samples with Fe content fixed at 40 at%.

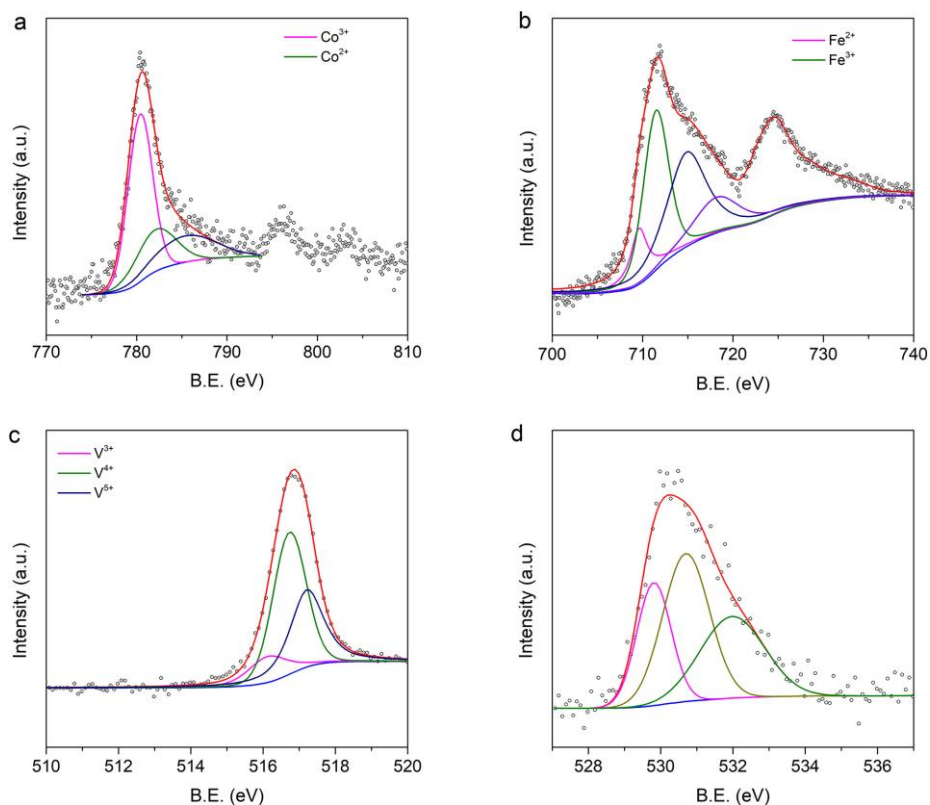


**Fig. S20** High-resolution XPS spectra of (a) Co, (b) Fe, and (c) V in  $\text{Co}_3\text{Fe}_4\text{V}_3\text{O}_x$  after the OER stability test.

**Table S8.** The valence state of metal species in  $\text{Co}_3\text{Fe}_4\text{V}_3\text{O}_x$  after the OER stability test determined from XPS analysis (in at%).

Conditions	$\text{Co}^{2+}$	$\text{Co}^{3+}$	$\text{Fe}^{2+}$	$\text{Fe}^{3+}$	$\text{V}^{3+}$	$\text{V}^{4+}$	$\text{V}^{5+}$
Before OER test	73.9	26.1	18.7	81.3	13.2	62.3	24.5
After OER test	29.0	71.0	14.6	85.4	2.3	20.1	77.5